Macromolecules
ARTICLE

Macromolecules **2010**, *43*, 7785–7792 **7785**
DOI: 10.1021/ma1012418

Synthesis, Characterization, and Long-Term Stability of Hollow Polymer Nanocapsules with Nanometer-Thin Walls

Sergey A. Dergunov,[†] Katrina Kesterson,[†] Wei Li,[‡] Zhao Wang,[‡] and Eugene Pinkhassik*,[†]

[†]*Institute for Nanomaterials Development and Innovation (INDIUM) and Department of Chemistry, The University of Memphis, 213 Smith Chemistry Building, Memphis, Tennessee 38152-3550, and* [‡]*Department of Pharmaceutical Sciences, the University of Tennessee Health Science Center, Memphis, Tennessee 38163*

Received June 3, 2010; Revised Manuscript Received August 4, 2010

ABSTRACT: Hollow polymer nanocapsules are produced by the polymerization within hydrophobic interior of lipid bilayers that act as temporary self-assembled scaffolds. Pore-forming templates are codissolved with monomers in the bilayers to create pores with controlled size and chemical environment. Polymerization was monitored with UV spectroscopy and dynamic light scattering. High-resolution magic angle spinning NMR characterization provided detailed structural information about nanocapsules. Spherical shape was confirmed by electron microscopy. Medium-sized molecules can be entrapped within porous nanocapsules. No release of encapsulated molecules was observed within 240 days.

Introduction

Hollow polymer capsules are important for diverse applications, e.g., drug delivery, nanoreactors, and sensors.[1−3] Controlling permeability and decreasing the thickness of nanocapsule walls are critical for successful applications. Recently, we reported preliminary results on the synthesis of polymer nanocapsules with nanometer-thin shells and imprinted nanopores with controlled size and chemical environment.[4,5] These capsules are capable of ultrafast transport of ions.[6]

The synthetic approach to the creation of nanocapsules with nanometer-thin walls is based on the controlled polymerization in the hydrophobic interior of lipid bilayers. Previously, vesicles made of lipids or ammonium salt-based surfactants were used to form polymer capsules.[7] In our work, hydrophobic templates are used to create nanopores.[4,5] This approach is an example of directed assembly of nanomaterials, where a covalent assembly of building blocks occurs within a self-assembled scaffold.[8] This general synthetic approach can be expanded to the synthesis of other nanostructures, e.g., polymer nanodisks.[9] Self-assembly of amphiphiles into aggregates of different morphologies has been of interest across biological, chemical, and physical sciences for several decades.[10] The directed assembly method is likely to be used for creating nanostructures with diverse shapes. The ability to control self-assembly in order to produce nanomaterials of desired morphology and properties is vital for development of future nanoscale technologies.[11]

Here we discuss the preparation of nanocapsules, their characterization with electron microscopy and NMR, and evaluation of long-term stability of nanocapsules in liquid suspensions.

Experimental Details

Chemicals. 1,2-Dimyristoyl-*sn*-glycero-3-phosphocholine (DMPC) was purchased from Avanti Polar Lipids, Inc., as a dry powder. Synthesis of glucose tetraacetate coupled with 4-vinylbenzoic acid[5] and Reactive Blue dye coupled with β-cyclodextrin[4] was described previously. All other chemicals and Sephadex G-50 were purchased from Sigma-Aldrich. Divinylbenzene (DVB) and *tert*-butylstyrene (TBS) were passed through alumina column to remove the inhibitor shortly before the polymerization. Sephadex G-50 (10 g) was swollen in 120 mL of water in a glass screw-capped bottle for at least 5 h at room temperature and stored at 4 °C until required for use. All other chemicals were HPLC grade and not further purified before use.

Preparation of Nanocapsules. *tert*-Butylstyrene (16 μL, 8.84×10^{-5} mol), *p*-divinylbenzene (13 μL, 8.84×10^{-5} mol), and photoinitiator 2,2-dimethoxy-2-phenylacetophenone (3 mg, 0.117×10^{-5} mol) were added to a chloroform solution of DMPC (8.84×10^{-5} mol, 60 mg/mL) or DMPC mixed with pore forming template (0.87×10^{-5} mol, in chloroform). Chloroform was evaporated using a stream of purified argon to form a lipid/monomer film on the walls of a culture tube. The lipid film was further dried under vacuum for 30 min to remove traces of chloroform. GC and UV−vis analysis confirmed that the concentration of monomers after drying remained the same. The dried film was hydrated with deionized water with or without dyes used as size probes giving a dispersion of multilamellar vesicles. The suspension was extruded 10 times at 32 °C through a polycarbonate Nucleopore track-etch membrane (Whatman) with 0.1 μm pore size using a Lipex stainless steel extruder (Northern Lipids). Typically, when dyes were used, nonentrapped dye molecules were removed by size-exclusion chromatography. A column was prepared by filling a disposable 3 mL syringe with 3 mL of hydrated Sephadex G-50. The column was placed in a culture tube and was spun in a bench centrifuge (VWR Clinical 50) at 2500 rpm for 3 min to remove excess of water. Liposome suspension (0.6 mL) was added dropwise onto the column. Column was then spun in a bench centrifuge at 2500 rpm for 5 min. Prior to the polymerization, oxygen was removed by passing purified nitrogen or argon through the solution. The sample was irradiated with UV light (λ = 254 nm) in a photochemical reactor (10 lamps, 32 W each; the distance between the lamps and the sample was 10 cm) using quartz tube with path length of light of ~3 mm. Short path length is important for efficient polymerization in the presence of dyes. Every 10 min, a 100 μL aliquot of the solution was taken for analysis. Experiments with varying monomer:lipid and monomer:cross-linker

*Corresponding author. E-mail: epnkhssk@memphis.edu.

Published on Web 08/16/2010

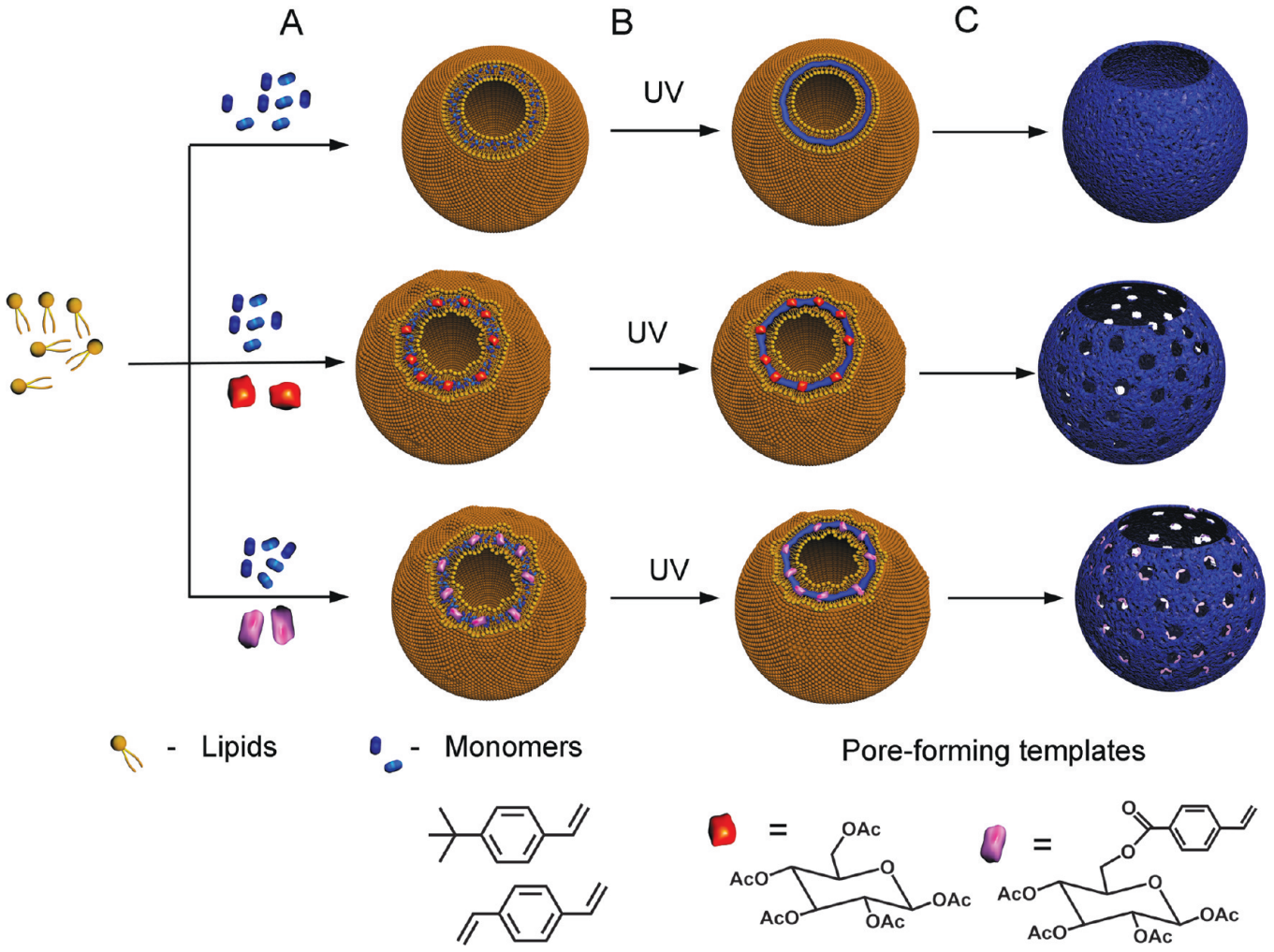

Figure 1. Scheme of nanocapsules formation: (A) formation of liposomes with loaded monomers (or monomers and pore-forming template molecules); (B) irradiation with UV light and formation of fortified liposomes; (C) lipid removal and formation of hollow nanocapsules with thin walls (and with pores if pore-forming template was used).

ratios were conducted in a similar manner. An aqueous solution of Procion Red dye was used to hydrate the lipid/monomer mixture. After the synthesis, samples were mixed with Triton X-100 and separated on a size-exclusion chromatography column (Sephadex G-50). Pore size was measured by a colored size probe retention assay as described previously.[4]

Dynamic Light Scattering (DLS). Hydrodynamic diameter and polydispersity index (PDI) measurements were performed on a Malvern Nano-ZS zetasizer (Malvern Instruments Ltd., Worcestershire, U.K.). The helium−neon laser, 4 mW, operates at 633 nm, with the scatter angle fixed at 173°, and the temperature at 25 °C. 80 μL samples were placed into disposable cuvettes without dilution (70 μL, 8.5 mm center height Brand UV-Cuvette micro). Each data point was an average of 10 scans.

UV−vis Spectroscopy. UV measurements were performed on a UV−vis photodiode array spectrophotometer (Agilent 8453 UV−vis spectrophotometer) using a quartz cuvette of 1 cm optical path length. 50 μL aliquots from the polymerization experiment were suspended in 1 mL of hexane to extract residual monomers.

Long-Term Stability Studies. Nanocapsules with entrapped Procion Red were suspended in methanol. Samples were stirred at different temperatures (6, 25, and 45 °C). A 400 μL aliquot of the supernatant solution was taken at regular intervals (every week for the first 120 days, every 20 days between 120 and 240 days) for analysis with a UV−vis photodiode array spectrophotometer (Agilent 8453 UV−vis spectrophotometer) using a quartz semi-microcuvette with 1 cm optical path length. After the measurement, the aliquot was returned to the sample.

Electron Microscopy. TEM images were acquired on a JEOL JEM1200EX II microscope at an acceleration of 100 kV. Samples were negatively stained with phosphotungstic acid (pH = 5.9) on a carbon grid. SEM images were obtained with a Philips XL 30 ESEM, coated with thick gold−palladium (60:40) layer using EMS 590 X sputter.

High-Resolution Magic Angle Spinning (HRMAS) NMR. ^{1}H HRMAS NMR experiments were carried out on a Varian 500 spectrometer equipped with a 4 mm gHX Nanoprobe (Variannmr Inc., Palo Alto, CA) in a similar fashion to the previously described method.[12] Briefly, samples were prepared by dispersing freeze-dried nanocapsules in deuterated solvents. The resulted suspensions were transferred to glass Nanoprobe rotors that have a total volume of 40 μL. Rotors were spun at 1500−2500 Hz with a general accuracy of ±2 Hz and optimized for each sample to minimize overlap of spinning side bands with peaks from nanocapsules. 1D ^{1}H NMR spectra were acquired with solvent suppression when needed. 2D NMR spectra were acquired using vendor supplied standard pulse sequences. Individual parameters were optimized for each sample. All spectra were acquired at 22 °C. Chemical shifts were calibrated to residual solvent peaks.

Results and Discussion

Synthesis. Polymer nanocapsules were synthesized by free radical photopolymerization of 4-*tert*-butylstyrene (TBS)

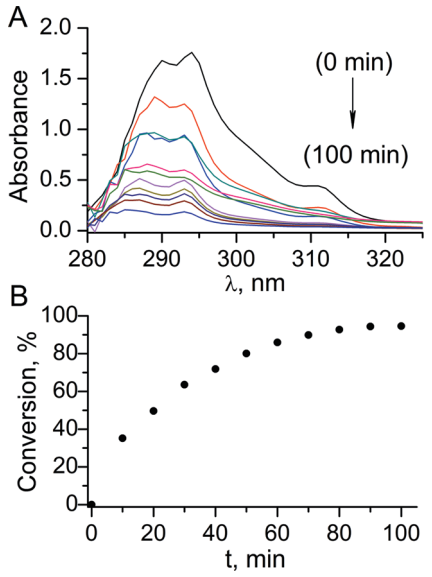

Figure 2. (A) Absorption spectra of monomers during polymerization (10 min intervals). (B) Percent conversion of monomers as a function of time.

with cross-linker *p*-divinylbenzene (DVB) with or without pore-forming molecules incorporated into the lipid bilayers (Figure 1). Removal of the phospholipid bilayer and pore-forming templates from the rigid polymer yields nanospheres with pores that are complementary to the original porogen. Two types of pore-forming templates were used. One kind consisted of hydrophobic inert molecules that did not participate in the polymerization and formed hydrophobic pores. Glucose pentaacetate and glucose pentabenzoate were used as inert templates.

The other type of template was made of a polymerizable moiety and a bulky pore-forming part joined by a degradable linker. Here we used a molecule prepared by the coupling of glucose tetraacetate with 4-vinylbenzoic acid.[5,13] 4-Vinylbenzoic moiety copolymerizes with TBS and DVB. After the capsule formation, the ester linker is broken by alkaline hydrolysis to yield nanopores containing a single carboxylic group. Pore sizes can be measured by a size-probe retention assay as previously described.[4,5]

UV spectra of monomers show a characteristic absorption at 290 nm corresponding to the $\pi \rightarrow \pi^*$ transition of the conjugated π system. Involvement of vinyl groups in the polymerization results in lowering of absorption in this spectral region. We used disappearance of absorption at 290 nm as the measure of polymerization (Figure 2A). Time-resolved UV measurements show that the polymerization is essentially complete within 1 h (Figure 2B). Further shortening of the polymerization time can be conceivably achieved by increasing intensity of irradiation, shortening the effective path length of light, or by optimizing the use of photochemical initiators.

To corroborate UV-based monitoring of polymerization and to gain further insight into polymerization, we used dynamic light scattering to examine the suspension during polymerization. For each time point, two aliquots were taken from solution. One was analyzed by DLS directly. The other was mixed with excess surfactant Triton X-100 (sufficient amount to lyze liposomes) and then analyzed with DLS. Samples that were analyzed without surfactant treatment showed no change in size and polydispersity (Figure 3A). We conclude that polymerization within the bilayers does not negatively affect the integrity of liposomes. Sample mixed

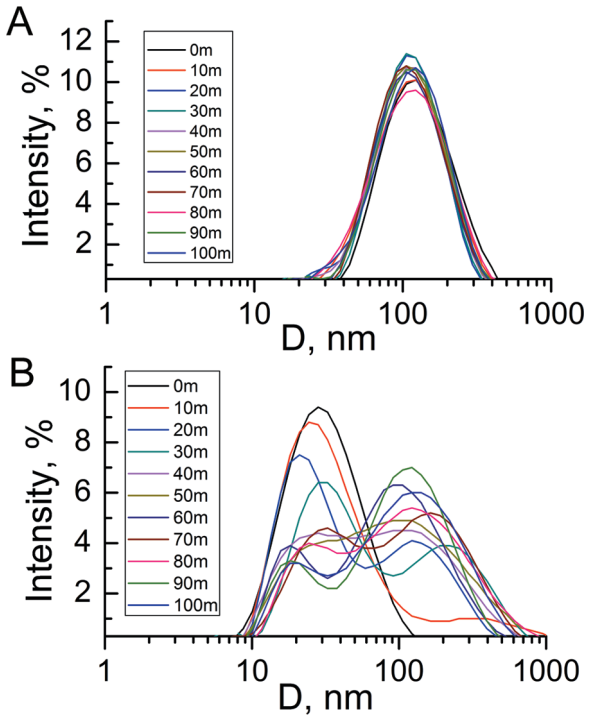

Figure 3. Size distribution of DMPC liposomes during synthesis (A) and after addition of TX100 (B).

with a surfactant prior to the polymerization shows that liposomes have been lyzed, and only Triton micelles are visible (Figure 3B, $t = 0$ min). Sample measured after 10 min of exposure to UV light revealed a small amount of larger particles, likely indicative of the formation of capsules. The sample measured after 20 min of polymerization showed a bimodal distribution with average sizes of approximately 20 and 100 nm. The particles with a diameter of ~20 nm correspond to the TX-100 and TX-100/lipid micelles that are formed after removal of lipids from the polymer network. The particles with a diameter about 100 nm indicate that the polymerization led to a stable and intact 2D network and that closed capsules formed. An open network with defects would not be stable without the lipid environment and would either collapse or deflate. Monitoring of polymerization (Figure 2) shows that in the 20 min sample ~50% of monomers were used up. DLS data strongly suggest that after 20 min a substantial amount of polymer capsules has been formed. The formation of nanocapsules was confirmed with TEM imaging as described below. All subsequent samples showed similar bimodal distribution with greater relative content of the 100 nm component.

In contrast to previous studies on polystyrene-containing vesicles,[14] in our system the structures do not noticeably change size during synthesis procedure. Importantly, the cross-linking does not modify the liposome size, and most of the particles kept the initial template size after the addition of detergent.

To compare the structure and properties of styrene-derived nanocapsules prepared from different monomer/lipid formulations, we varied the monomer:lipid and monomer:cross-linker ratios. In this work, we focused on nanocapsules prepared from styrene derivatives. Previously, we examined loading of monomers into different lipids and found little difference in loading capacity of saturated lipids above their phase transition temperature.[8b] We therefore chose DMPC as the representative lipid. We also found that the loading capacity did not change with the size of the liposome,[8a] and we selected

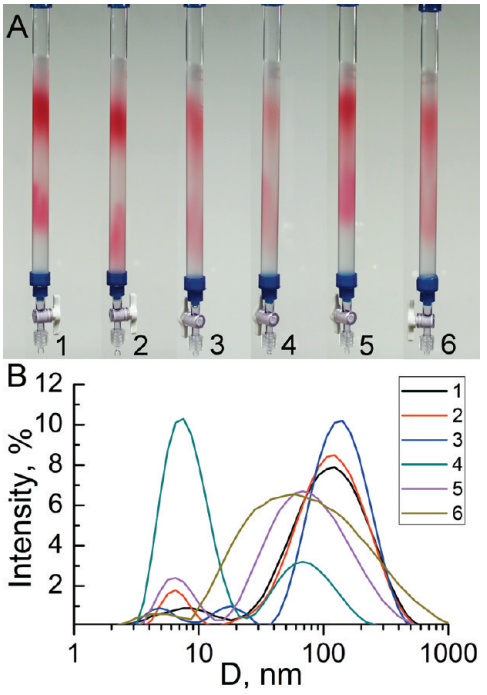

Figure 4. Permeability and DLS study of nanocapsules prepared by varying monomer:lipid (M:L) and monomer:cross-linker (M:C) ratios. Sample 1: M:L = 3:1, M:C = 1:1; sample 2: M:L = 2:1, M:C = 1:1; sample 3: M:L = 1:1, M:C = 1:1; sample 4: M:L = 0.5:1, M:C = 1:1; sample 5, M:L = 3:1, M:C = 10:1; sample 6: M:L = 3:1, no cross-linker. (A) Size-exclusion separations of samples after polymerization and treatment with surfactant. Liposomes were prepared in the presence of Procion Red (MW 615). Nonentrapped dye was not separated prior to the polymerization. (B) DLS measurements after the polymerization, treatment with surfactant, and size-exclusion separation.

liposomes prepared by extrusion through a 0.1 μm filter as the template for nanocapsule assembly. The synthesis was performed as described above. Liposomes were formed in the presence of Procion Red dye (MW 615, smallest cross section 1.1 nm) to evaluate the retention of medium-sized molecules in the polymer nanocapsules. After 90 min of UV irradiation of the liposomes loaded with monomers, the samples were mixed with Triton X-100, analyzed with DLS and TEM, and separated from nonentrapped dyes on a size-exclusion column.

In these experiments, the dye was not separated from liposomes prior to the polymerization. This was done to simplify the observation of retention of dyes within the nanocapsules. In this setup, the bulk of the dye was not encapsulated within the liposomes. Following the polymerization, the sample was mixed with a surfactant, which would lyze liposomes and release the dye molecules. Nanocapsules, solubilized with surfactant molecules, would elute faster than free dye. If dye is retained within the nanocapsules, the nanocapsule fraction can be easily observed on the column.

When using 1:1 monomer:cross-linker ratio, nanocapsules were able to retain entrapped dyes as evidenced by the separation on a size-exclusion column (Figure 4A, samples 1−4; monomer:lipid ratio 3:1, 2:1, 1:1, and 0.5:1, respectively). Eluted fractions were analyzed with DLS and TEM. DLS data show that nanocapsules prepared with 1:1 monomer:cross-linker ratio and monomer:lipid ratio between 3:1 and 1:1 show nanocapsules with ~100 nm diameter (Figure 4B, samples 1−3). DLS data show bimodal distribution for each of these samples with the predominant scattering from larger particles (nanocapsules) and less intense scattering from smaller particles (surfactant micelles). Formation of 100 nm nanocapsules was confirmed with TEM imaging as described below. Monomer:lipid ratio of 0.5:1 (1:1 monomer:cross-linker ratio) also showed bimodal distribution in DLS showing greater relative content of surfactant micelles and smaller diameter of nanocapsules (60−70 nm) than the samples above (Figure 4B, sample 4). TEM data, discussed below, showed smaller nanocapsules. Since all samples were prepared under identical conditions and treated with the

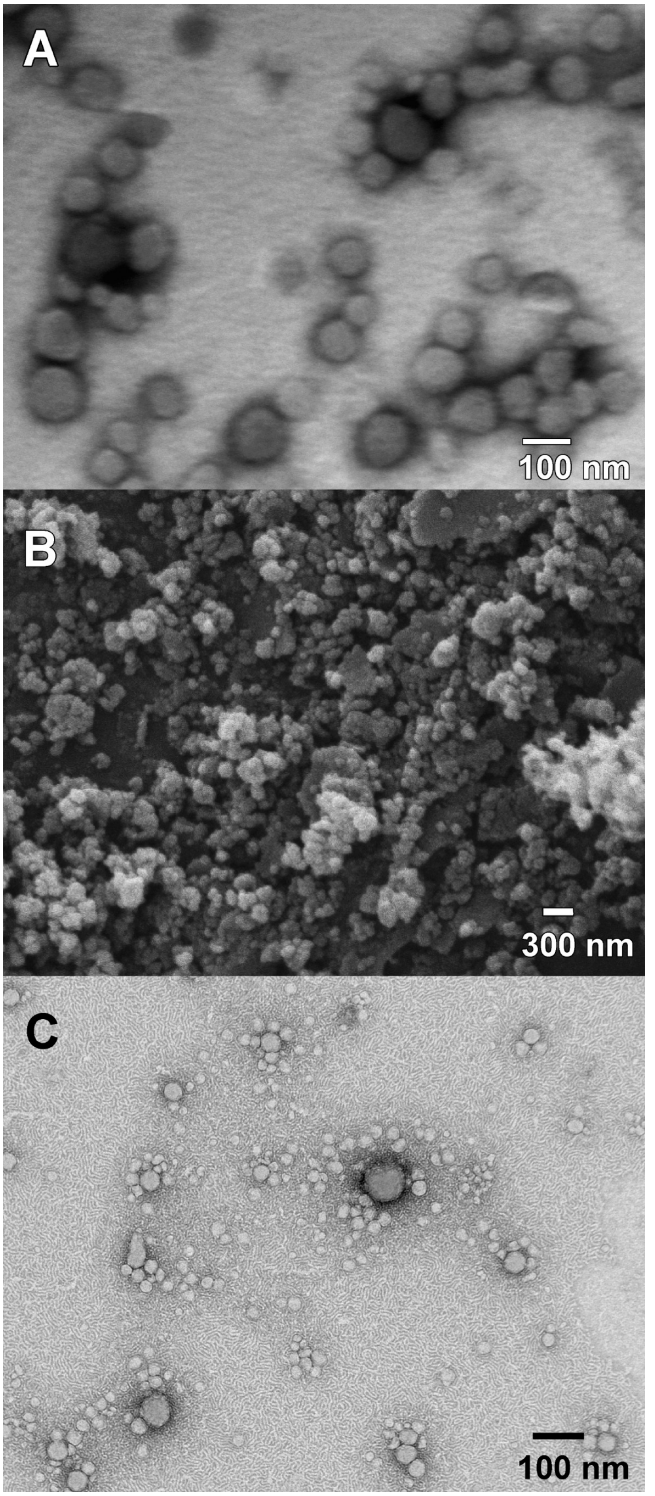

Figure 5. Electron micrograph of nanocapsules. TEM (A) and SEM (B) images of nanocapsules after polymerization and removal of lipid scaffold with methanol. (C) TEM image of an aliquot from the reaction mixture taken after 20 min of UV exposure and treated with Triton X-100.

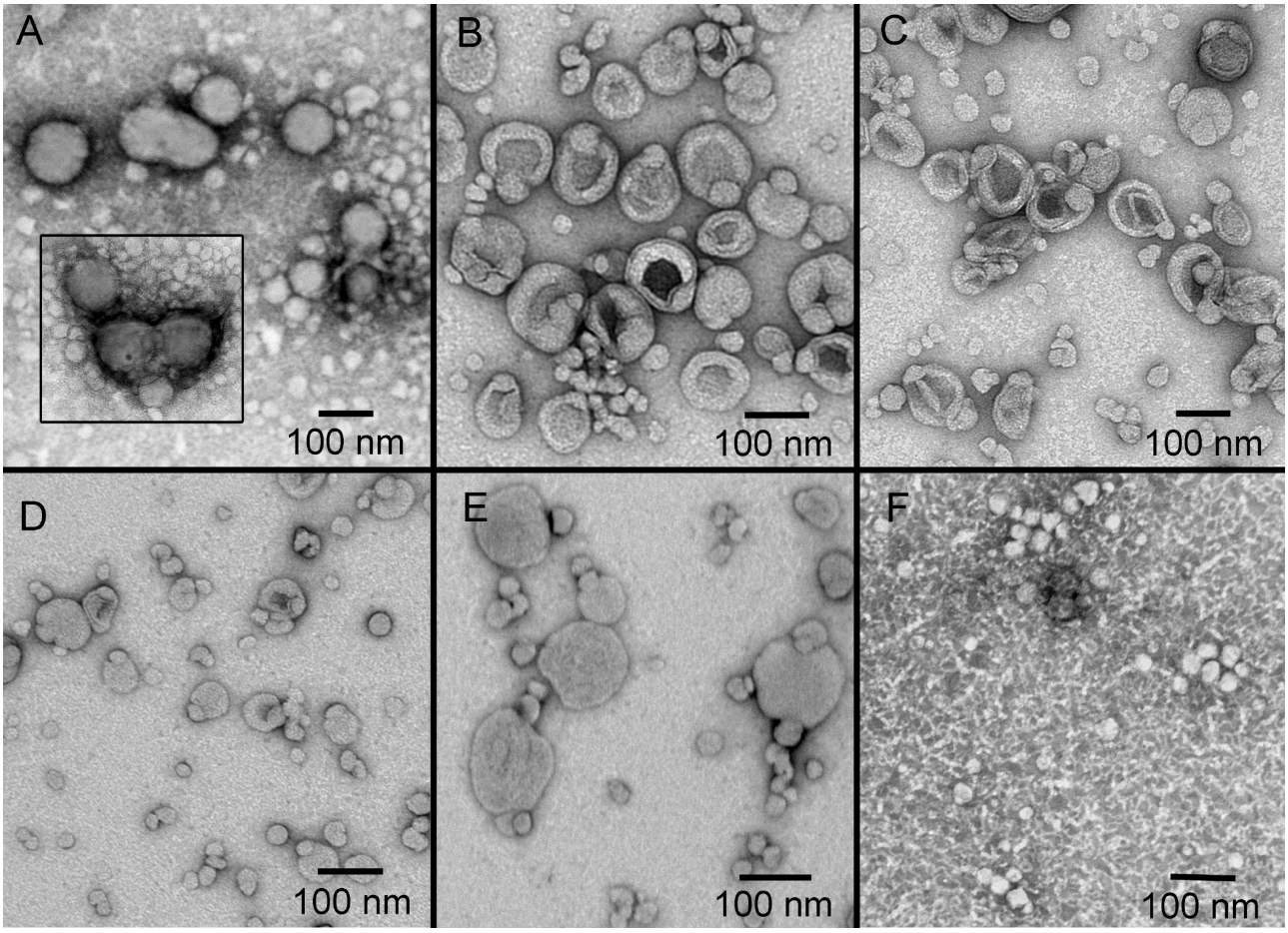

Figure 6. TEM images of nanocapsules prepared by varying monomer:lipid (M:L) and monomer:cross-linker (M:C) ratios. In these experiments, liposomes loaded with monomers were irradiated with UV light for 90 min and treated with Triton X-100. (A) M:L = 3:1, M:C = 1:1; (B) M:L = 2:1, M:C = 1:1; (C) M:L = 1:1, M:C = 1:1; (D) M:L = 0.5:1, M:C = 1:1; (E) M:L = 3:1, M:C = 10:1; (F) M:L = 3:1, no cross-linker.

same amount of surfactant, the low relative scattering intensity at 60−70 nm in sample 4 suggests that only a small amount of nanocapsules is formed when using 0.5:1 monomer:lipid ratio.

Sample prepared with 10:1 monomer:cross-linker ratio (Figure 4, sample 5; 3:1 monomer:lipid ratio) showed a broad size distribution with the 70−80 nm average. These capsules were not able to retain Procion Red dye. Higher permeability of these capsules is expected because lower amount of cross-linker should result in larger inherent pores in the capsule walls. In addition, such capsules should exhibit higher conformational flexibility. Consequently, removal of lipids with a surfactant is likely to result in deformation of nanocapsules, resulting in smaller apparent size observed in DLS.

In a control experiment, we polymerized TBS in the absence of DVB cross-linker within the bilayer (Figure 4, sample 6; 3:1 monomer:lipid ratio). Again, no retention of Procion Red dye was observed. DLS data showed a very broad size distribution, likely arising from different aggregates of linear polymers. No capsules were observed in TEM as shown below. Clearly, the presence of a cross-linker is essential for creating nanocapsules in the bilayer interior.

Electron Microscopy. Transmission electron microscopy (TEM) characterization confirmed the formation of uniform polymer nanocapsules (Figure 5A). TEM images of freeze-dried nanocapsules prepared using 1:1 monomer:cross-linker ratio and 3:1 monomer:lipid ratio were virtually identical to the images of liposomes used for templating nanocapsules. TEM revealed no structures with different morphology, such as parachute-like objects,[15] than those shown in Figure 5A.

Scanning electron microscopy (SEM) showed that freeze-dried nanocapsules preserved their spherical shape (Figure 5B). This finding differs from a previous observation by Jung et al of parachute-like structures produced from vesicle-templated polymerization of acrylates.[15] Two important differences may account for higher stability of nanocapsules described here. First, we used styrene derivatives, which are less conformationally flexible than butyl methacrylate and ethyele glycol dimethacrylate used in other studies. Second, the aspect ratio of capsule diameter to wall thickness is much smaller in 100 nm capsules than in micrometer-sized vesicles used in other reports.

Varying monomer:lipid and monomer:cross-linker ratios resulted in nanocapsules with different structures. Figure 6 shows the TEM images obtained after loading DMPC liposomes with different formulations of monomers, irradiating samples for 90 min with UV light and removing the lipid scaffold with Triton X-100. Samples A−F in Figure 6 correspond to samples 1−6 in Figure 4. Lowering monomer:lipid ratio to 2:1 or 1:1 resulted in nanocapsules that appear collapsed in TEM (Figure 6B,C). The average size of these structures is ~100 nm, the same as liposomes used for templating and nanocapsules formed with 3:1 monomer:lipid ratio. These observations are in agreement with previously reported data for acrylate-based nanocapsules.[15] Apparently, the wall thickness is linked to the mechanical stability of nanocapsules. While nanocapsules in Figure 6B,C collapsed upon drying in vacuum, removal of lipid scaffold with

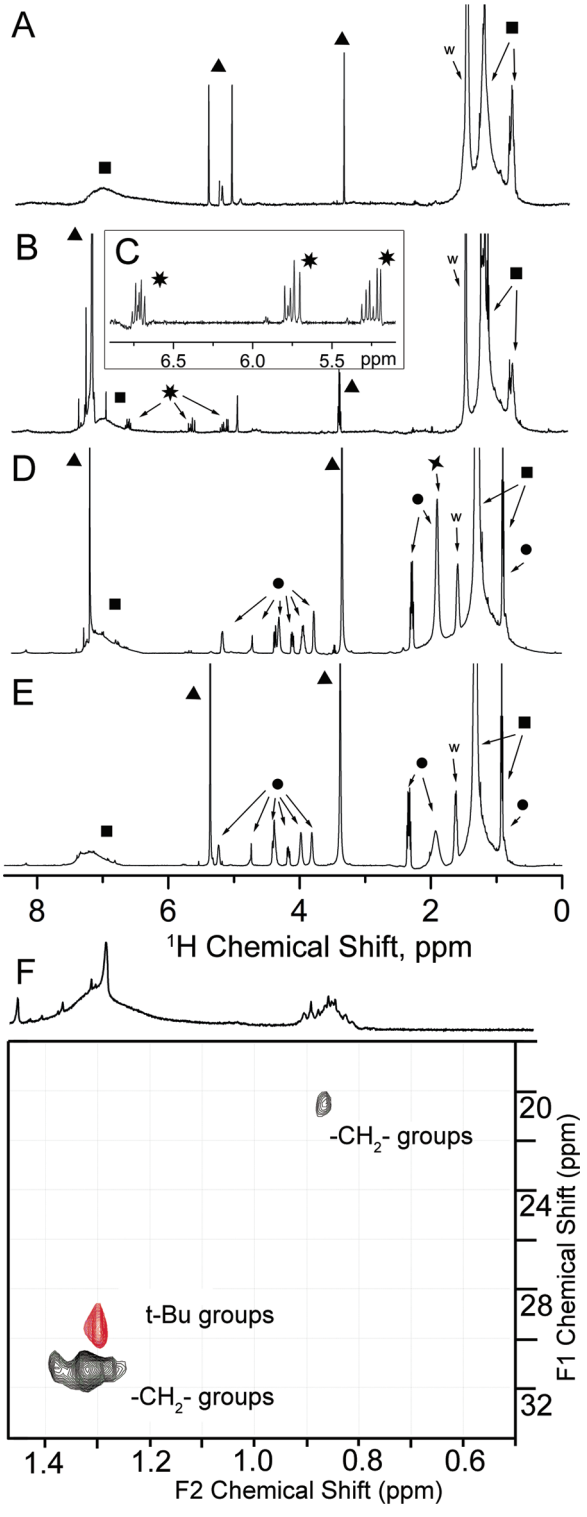

Figure 7. MAS NMR spectra of the nanocapsules (A) after synthesis and washing with methanol and (B) after synthesis, washing, and hydrolysis with NaOH. (C) Inset region of vinyl groups. (D) and (E) show nanocapsules with and without pore-forming template after precipitation in methanol. (F) Two-dimensional proton−carbon HSQC spectrum. Descriptions: ▲, solvents; ■, polymers; ●, lipid; ∗, vinyl groups from the polymer; W = water; X = acetyl groups from pore-forming template.

surfactants did not lead to the release of the entrapped content as shown by size-exclusion chromatography (Figure 4A, samples 2 and 3). These results are helpful for choosing appropriate handling methods in practical applications of nanocapsules.

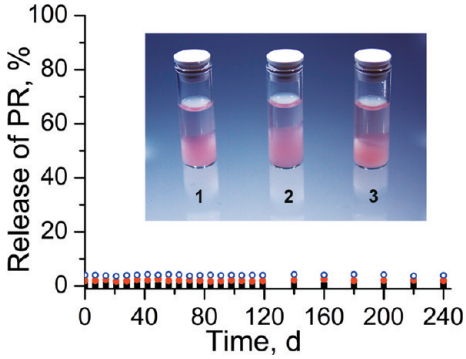

Figure 8. Long-term stability of nanocapcules and retention of Procion Red in polymer nanocapsules. Capsules with Procion Red stored in refrigerator (sample 1, ■), at room temperature (sample 2, ●), and at 45 °C (sample 3, ○). Data points were offset for clarity.

Nanocapsules prepared with 0.5:1 monomer:lipid ratio (Figure 6D) are smaller on average than those formed from higher monomer:lipid ratios and are smaller than liposomes used for templating. The amount of monomers solubilized within the bilayer is clearly too small to form the same kind of nanocapsule as shown in Figure 6A−C. Indeed, with 0.5:1 monomer:lipid ratio, an average of one monomer molecule is sandwiched between a pair of lipids that occupy 0.63 nm^2. At the same time, most structures in Figure 6D are circular, suggesting that they possessed spherical shape before drying. It is conceivable that removal of lipid scaffold with surfactants and aqueous exposure caused shrinking of hydrophobic nanocapsules. The similarity between these capsules and those formed after 20 min of UV irradiation of liposomes with 3:1 monomer:lipid ratio (Figure 5C) further supports the above conclusions. Many nanocapsules are not fully formed after 20 min of polymerization as evident from data presented in Figure 3, and removal of lipids may have also caused shrinkage of those structures.

Using 10:1 monomer:cross-linker ratio yields structures that appear slightly larger than 100 nm on average in TEM (Figure 6E) and smaller than 100 nm in DLS (Figure 4B, sample 5). A likely explanation is that due to smaller amount of a cross-linker, these nanocapsules are softer than those prepared with 1:1 monomer:cross-linker ratio, and they dry to form flat structures resembling pita bread rather then collapsed brittle hemispheres. Because 3:1 monomer:lipid ratio was used to prepare these capsules, their walls are too thick for capsules to shrink. Flattened structures should appear smaller in DLS due to their higher mobility. These nanocapsules showed no retention of entrapped Procion Red, in agreement with larger inherent pore size and higher conformational flexibility of capsule walls compared with capsules prepared with 1:1 monomer:cross-linker ratio.

Polymerization of TBS in the absence of DVB cross-linker in the bilayer interior did not result in the formation of nanocapsules (Figure 6F). The TEM image reveals only Triton and Triton/lipid micelles and random polymers.

HRMAS NMR. To gain further insight into chemical composition of nanocapsules, capsules were analyzed with high-resolution magic angle spinning (HRMAS) NMR. Samples were prepared by dispersing freeze-dried nanocapsules in deuterated solvents. We tested spectral resolution and intensity using a variety of NMR solvents and found that CD_3Cl or CD_2Cl_2 provided the best overall performance. CD_2Cl_2 is slightly better than CD_3Cl for these samples because it has less interference to NMR peaks in the aromatic region, although it is much more volatile. Polystyrene structure

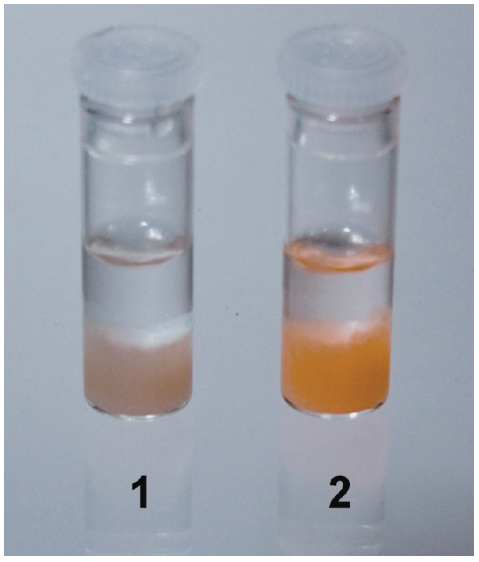

Figure 9. pH-dependent response of nanocapsules with encapsulated Congo Red in methanol. Sample 1 is at pH 2; sample 2 is at pH 5.

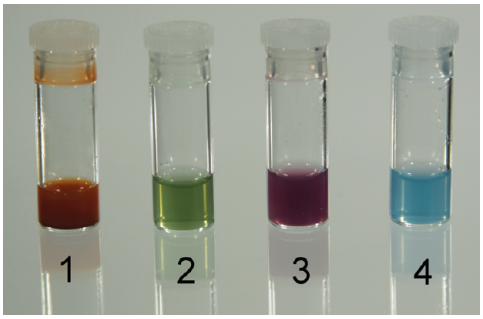

Figure 10. Pore size measurement by colored size probe retention assay. Samples 1 and 2 show nanocapsules before removal of pore-forming templates (glucose tetraacetate coupled with 4-vinylbenzoic acid); samples 3 and 4 show capsules after the removal of pore-forming template by alkaline hydrolysis. Nanocapsules in sample 1 contain a mixture of methyl orange (yellow, smallest cross section 0.6 nm), Procion Red (red, smallest cross section 1.1 nm), and Reactive Blue coupled with β-cyclodextrin (blue, smallest cross section 1.6 nm). Sample 2 contains entrapped yellow and blue probes. In both cases, 0.6 nm probe is released, while 1.1 and/or 1.6 nm probes are retained.

is evident from a combination of aromatic and aliphatic protons in the ^{1}H NMR spectrum of nanocapsules after extended washing with methanol (Figure 7A). The ^{1}H NMR spectrum of nanocapsules after precipitation from methanol and minimal washing shows that phospholipids are present (Figure 7D). The presence of the inner layer of lipids is expected when the polymerization is performed in the absence of pore-forming templates.

We next wanted to obtain the ratio of *tert*-butyl protons to those of aromatic protons. While the aromatic protons are well isolated, protons in the *tert*-butyl group from monomers ($\sim$1.3 ppm) severely overlap with methylene protons from lipids in the 1D NMR spectra. This overlap prevented reliable quantification for protons in the *tert*-butyl group. To circumvent this problem, we performed DEPT (distortionless enhancement by polarization transfer) edited two-dimensional proton-carbon HSQC (heteronuclear single quantum correlation) experiment (Figure 7F). Signals from the *tert*-butyl group in this 2D measurement were well separated from those of the lipid methylenes in the carbon dimension. The ratio of *tert*-butyl to aromatic protons was then calculated reliably by combining the analysis of 1D and 2D HRMAS NMR spectra of the nanocapsules.

On the basis of integrals of the *tert*-butyl group and aggregate intensity of aromatic hydrogens (a sum of hydrogens from TBS and DVB), we calculate the TBS:DVB molar ratio in the nanocapsules to be 2:1. The TBS:DVB ratio loaded into the bilayers was 1:1, and the lower amount of DVB found in the nanocapsules is likely to be a reflection of its lower reactivity. On the basis of relative intensities of *tert*-butyl signal and signals from lipids and taking into account the TBS:DVB ratio, we calculated the monomers:lipids ratio to be approximately 6:1. This ratio suggests that after minimal washing more than half of lipids from the inner leaflet remain entrapped within the nanocapsules. No lipids were found in capsules after extensive washing with methanol (Figure 7A) or alkaline hydrolysis (Figure 7B).

The spectrum of nanocapsules after treatment with sodium hydroxide (Figure 7B) shows signals in the 5.2−6.8 ppm range (Figure 7C) corresponding to the vinyl groups. These vinyl groups are apparently nonreacted groups from divinylbenzene. It is highly unlikely that nonreacted TBS or DVB molecules are still present because the materials are only 1−2 nm thick and capsules have been thoroughly washed with methanol. The most likely explanation is that one vinyl group of DVB was involved in the polymerization and the other vinyl group did not react because there were no more monomers in the close proximity available for the reaction.[16] Integration of vinyl peaks and comparison with aromatic hydrogens revealed the molar ratio of approximately 1:20. These vinyl groups may open opportunities for further functionalization. For example, one can copolymerize nanocapsules with styrene, effectively linking capsules together. Another possibility is to perform an electrophilic addition (e.g., HBr) and use the resulting derivative for subsequent transformations.

Long-Term Stability of Nanocapsules. To evaluate long-term stability of nanocapsules, we examined retention of medium-sized molecules in a liquid suspension−the most likely mode of nanocapsule applications. We used Procion Red (MW 615, smallest cross section 1.1 nm) entrapped within nanocapsules as the probe. In these experiments, suspensions of nanocapsules containing Procion Red were stirred at different temperatures: 6, 25, and 45 °C. Each week, an aliquot was taken from the sample, and the UV spectrum was recorded. After the first 120 days, UV measurements were done every 20 days. To achieve low detection limit, the solutions were not diluted for the measurements. With this method, concentration of Procion Red corresponding to the release of 1% or more of the entrapped dye would be detected. No measurable release of Procion Red was observed during 240 days (Figure 8).

Retention of medium-sized molecules can be used for practical applications, such as optical sensors or nanoreactors. For example, a pH-sensitive indicator dye Congo Red undergoes a color transition in the pH range of 3−5. To demonstrate the feasibility of using nanocapsules to immobilize indicator dyes, we entrapped Congo Red in nanocapsules. As in the case with Procion Red, described above, we did not observe release of Congo Red for an extended period of time. Changing the pH from acidic to neutral is accompanied by immediate color change (Figure 9).

Pore sizes of nanocapsules were measured by a colored size probe retention assay as described previously.[4] Briefly, a mixture of dyes with different cross sections and different UV−vis spectra are entrapped in liposomes containing monomers and pore-forming templates in the bilayer interior. After the polymerization and template removal, surfactant-solubilized nanocapsules are separated by size-exclusion

chromatography. Size probes with the cross section smaller than the pore size escape from the nanocapsule and are separated on a column. Analysis of the nanocapsule fraction shows which size probes remain entrapped within the nanocapsules. In this work, when using glucose pentaacetate and glucose tetraacetate coupled with 4-vinylbenzoic acid, pore sizes were found to be between 0.6 and 1.1 nm (Figure 10).

Summary

Controlled polymerization within hydrophobic interior of lipid vesicles is a convenient method for the synthesis of hollow nanocapsules. HRMAS NMR provided important structural information on nanocapsules. A 2:1 ratio of TBS to DVB was determined from the NMR spectra. Presence of inner leaflet of lipids was shown in the nanocapsule samples measured after minimal processing. Extensive washing of nanocapsules with methanol or treatment with sodium hydroxide removed all lipids. A small amount of residual vinyl groups was found in nanocapsules, opening opportunities for further functionalization or covalent linking of nanocapsules. Incorporation of pore-forming templates into nanocapsule walls and their removal upon alkaline hydrolysis was also confirmed by NMR.

Varying monomer:lipid and monomer:cross-linker ratios affected permeability and structures of resulting nanocapsules. Nanocapsules prepared from building blocks loaded into the bilayer interior at 3:1 total monomer:lipid and 1:1 monomer: cross-linker ratios retain their spherical shape upon drying. Smaller amounts of monomers loaded into the bilayer lead to nanocapsules that collapse upon drying. Regardless of their structural stability toward drying in vacuum, nanocapsules prepared with high content of a cross-linker are capable of retaining medium-sized molecules. Small relative amount of a cross-linker yielded softer nanocapsules that release medium-sized molecules. In the absence of a cross-linker no nanocapsules were observed upon removal of the lipid scaffold.

Nanocapsules showed excellent long-term stability. No medium-sized molecules were released from nanocapsules over an 8 month period. A pH-sensitive indicator dye was entrapped and was shown to change color upon changing pH of the solution. These findings enhance the directed assembly technology for the synthesis of nanocapsules and set the stage for practical applications such as nanoreactors or optical sensors.

Acknowledgment. This work was supported by NSF grants (CHE-0349315 and CHE-1012951), National Institutes of Health grant (1R01HL079147-01), FedEx Institute of Technology Innovation Award, CIBA foundation, and funds from College of Pharmacy, the University of Tennessee Health Science Center.

References and Notes

(1) (a) Sukhorukov, G. B.; Rogach, A. L.; Zebli, B.; Liedl, T.; Skirtach, A. G.; Köhler, K.; Antipov, A. A.; Gaponik, N.; Susha, A. S.; Winterhalter, M.; Parak, W. J. *Small* **2005**, *1* (2), 194–200. (b) Sukhorukov, G. B.; Rogach, A. L.; Garstka, M.; Springer, S.; Parak, W. J.; Muñoz-Javier, A.; Kreft, O.; Skirtach, A. G.; Susha, A. S.; Ramaye, Y.; Palankar, R.; Winterhalter, M. *Small* **2007**, *3* (6), 944–955. (c) Bédard, M. F.; Munoz-Javier, A.; Mueller, R.; del Pino, P.; Fery, A.; Parak, W. J.; Skirtach, A. G.; Sukhorukov, G. B. *Soft Matter* **2009**, *5*, 148–155. (d) Antipov, A. A.; Sukhorukov, G. B. *Adv. Colloid Interface Sci.* **2004**, *111*, 49–61. (e) De Geest, B. G.; Skirtach, A. G.; Mamedov, A. A.; Antipov, A. A.; Kotov, N. A.; De Smedt, S. C.; Sukhorukov, G. B. *Small* **2007**, *3* (5), 804–808.

(2) (a) Perkin, K. K.; Turner, J. L.; Wooley, K. L.; Mann, S. *Nano Lett.* **2005**, *5* (7), 1457–1461. (b) Brazel, C. S. *Pharm. Res.* **2009**, *26* (3), 644–656.

(3) (a) Delaittre, G.; Reynhout, I. C.; Cornelissen, J. J. L. M.; Nolte, R. J. M. *Chem.—Eur. J.* **2009**, *15*, 12600–12603. (b) Kim, K. T.; Cornelissen, J. J. L. M.; Nolte, R. J. M.; van Hest, J. C. M. *Adv. Mater.* **2009**, *21*, 2787–2791. (c) van Dongen, S. F. M.; de Hoog, H.-P. M.; Peters, R. J. R. W.; Nallani, M.; Nolte, R. J. M.; van Hest, J. C. M. *Chem. Rev.* **2009**, *109*, 6212–6274.

(4) Danila, D. C.; Banner, L. T.; Karimova, E. J.; Tsurkan, L.; Wang, X.; Pinkhassik, E. *Angew. Chem., Int. Ed.* **2008**, *47*, 7036–7039.

(5) Dergunov, S. A.; Pinkhassik, E. *Angew. Chem., Int. Ed.* **2008**, *47*, 8264–8267.

(6) Dergunov, S. A.; Miksa, B.; Ganus, B.; Lindner, E.; Pinkhassik, E. *Chem. Commun.* **2010**, *46*, 1485–1487.

(7) (a) Ruysschaert, T.; Germain, M.; Gomes, J. F. P.; da, S.; Fournier, D.; Sukhorukov, G. B.; Meier, W.; Winterhalter, M. *IEEE T. Nanobiosci.* **2004**, *3* (1), 49–55. (b) Ki, C. D.; Chang, J. Y. *Macromolecules* **2006**, *39*, 3415–3419.

(8) (a) Dergunov, S. A.; Schaub, S.; Richter, A. G.; Pinkhassik, E. *Langmuir* **2010**, *26*, 6276–6280. (b) Banner, L. T.; Danila, D. C.; Sharpe, K.; Durkin, M.; Clayton, B.; Anderson, B.; Richter, A. G.; Pinkhassik, E. *Langmuir* **2008**, *24*, 11464–11473.

(9) Tekobo, S.; Pinkhassik, E. *Chem. Commun.* **2009**, 1112–1114.

(10) (a) Ringsdorf, H.; Schlarb, B.; Venzmer, J. *Angew. Chem.* **1988**, *100*, 117. (b) Zhang, L.; Eisenberg, A. *Science* **1995**, *268*, 1728. (c) Jenekhe, S. A.; Chen, X. L. *Science* **1998**, *279*, 1903. (d) Meier, W. *Chem. Soc. Rev.* **2000**, *29*, 295.

(11) (a) Cheng, Zh.; D'Ambruoso, G. D.; Aspinwall, C. A. *Langmuir* **2006**, *22*, 9507. (b) Gomes, J. F. P. d. S.; Sonnen, A. F.-P.; Kronenberger, A.; Fritz, J.; Coelcho, M. Á. N.; Fournier, D.; Fournier-Nöel, C.; Mauzac, M.; Winterhalter, M. *Langmuir* **2006**, *22*, 7755. (c) Krafft, M. P.; Schieldknecht, L.; Marie, P.; Giulieri, F.; Schmutz, M.; Poulain, N.; Nakache, E. *Langmuir* **2001**, *17*, 2872. (d) Lawson, G. E.; Lee, Y.; Singh, A. *Langmuir* **2003**, *19*, 6401. (e) Germain, M.; Grube, S.; Carriere, V.; Richard-Foy, H.; Winterhalter, M.; Fournier, D. *Adv. Mater.* **2006**, *18*, 2868.

(12) Zhou, H.; Du, F.; Li, X.; Zhang, B.; Li, W.; Yan, B. *J. Phys. Chem. C* **2008**, *112* (49), 19360–19366.

(13) (a) Neises, B.; Steglich, W. *Angew. Chem., Int. Ed. Engl.* **1978**, *17*, 522. (b) Hu, X.; Chen, H.; Zhang, X. *Angew. Chem., Int. Ed. Engl.* **1999**, *38*, 3518.

(14) Kurja, J.; Nolte, R. J. M.; Maxwell, I. A.; German, A. L. *Polymer* **1993**, *34*, 2045.

(15) (a) Jung, M.; Robinson, B. H.; Steytler, D. C.; German, A. L.; Heenan, R. K. *Langmuir* **2002**, *18* (7), 2873–2879. (b) Jung, M.; van Casteren, I.; Monteiro, M. J.; van Herk, A. M.; German, A. L. *Macromolecules* **2000**, *33* (10), 3620–3629. (c) Jung, M.; Hubert, D. H. W.; van Veldhoven, E.; Frederik, P.; van Herk, A. M.; German, A. L. *Langmuir* **2000**, *16* (7), 3165–3174.

(16) (a) Zhengpu, Zh.; Hodge, P.; Stratford, P. W. *React. Polym.* **1991**, *15*, 71–77. (b) Ishizu, K.; Gamoo, Sh.; Fukutomi, T.; Kakurai, T. *Polym. J.* (*Tokyo, Jpn.*) **1980**, *12* (6), 399–404.